Structural, electric and dielectric properties of Eu-doped SrBi$_2$Nb$_2$O$_9$ ceramics obtained by co-precipitation route

Mohamed Afqir[1,2,*], Amina Tachafine[2], Didier Fasquelle[2], Mohamed Elaatmani[1], Jean-Claude Carru[2], Abdelouahad Zegzouti[1], Mohamed Daoud[1], Salaheddine Sayouri[3], Taj-dine Lamcharfi[3], Mohamed Zouhairi[3]

[1]*Laboratoire des Sciences des Matériaux Inorganiques et leurs Applications, Faculté des Sciences Semlalia, Université Cadi Ayyad, Marrakech, Morocco*

[2]*Unité de Dynamique et Structure des Matériaux Moléculaires, Université du Littoral-Côte d'Opale, Calais, France*

[3]*Université Sidi Mohamed Ben Abdellah, Fès, Morocco*

Abstract

This paper presents a study of the structure and dielectric properties of Eu-doped SrBi$_2$Nb$_2$O$_9$ ceramics prepared by co-precipitation route and sintered at 850 °C. The materials were examined using XRD and FTIR methods. XRD data indicated the formation of well crystallized structure of the pure and doped SrBi$_2$Nb$_2$O$_9$, without the presence of undesirable phases. FTIR spectra do not bring a significant shift in the band positions. Moreover, the AC conductivity, dielectric constant and dielectric loss of the ceramics were determined through the frequency range [50 kHz–1 MHz]. In particular, the dielectric constant (ε') and dielectric losses ($\tan\delta$) of the SrBi$_2$Nb$_2$O$_9$ and SrBi$_{1.6}$Eu$_{0.4}$Nb$_2$O$_9$ ceramics were measured as a function of temperature at various frequencies.

Keywords: SrBi$_2$Nb$_2$O$_9$, Eu-doping, co-precipitation, dielectric properties

I. Introduction

The Aurivillius phases can be described by the following formula: $[Bi_2O_2]^{2+}[A_{m-1}B_mO_{3m+1}]^{2-}$, where m is the number of the pseudo-perovskite octahedrons interleaved between the Bi$_2$O$_2$ layers, A and B are cations in a 12 and 6-fold coordination, respectively [1,2]. SrBi$_2$Nb$_2$O$_9$ and SrBi$_2$Ta$_2$O$_9$ as members of $[Bi_2O_2]^{2+}[A_{m-1}B_mO_{3m+1}]^{2-}$ family of compounds with $m = 2$ consists of $[Bi_2O_2]^{2+}$ layers interleaved with $[Sr_{m-1}Nb_mO_{3m+1}]^{2-}$ perovskite-type layers. These materials are potential candidates for use in ferroelectric nonvolatile random access memories (FRAM), because of their excellent ferroelectric properties (excellent fatigue resistance, high Curie temperature) [3]. However, they suffer from higher dielectric loss due to the volatiliza-

tion of bismuth. In this regard, many efforts have been suggested doping by rare earth elements [4–6]. We found that the dielectric constant, the phase transition temperature (T_C) and dielectric loss decrease when bismuth is substituted with samarium or gadolinium [7,8]. Recently, fluorescence properties of Eu^{3+} ions incorporated into SrBi$_2$Nb$_2$O$_9$ have been studied by Volanti *et al.* [9]. In their work, Eu-doped SrBi$_2$Nb$_2$O$_9$ samples were prepared by the polymeric precursor method and their thermal, structural and morphological properties were characterized. The experimental results reveal that at certain temperatures, photoluminescence emissions in a visible light region are clearly observed for SrBi$_2$Nb$_2$O$_9$ doped by Eu^{3+}. This property has been proven to be extremely sensitive to short-, medium-, and long-range order in materials.

We are not aware of any study for the structural, electrical and dielectric properties of Eu-doped SrBi$_2$Nb$_2$O$_9$ ceramics. In addition, the high doping level (i.e. up

* Corresponding author: tel: +2126 42 37 94 83,
e-mail: *mohamed.afqir@yahoo.fr*

to 40 mol% Eu_2O_3) cannot be obtained by the solid state method. Because of these facts we chose the co-precipitation route to synthesize $SrBi_{2-x}Nb_2O_9$ ($x = 0$, 0.4) ceramics. Various characteristics of the obtained samples are reported, including dielectric properties.

II. Experimental

The pure and Eu-doped $SrBi_2Nb_2O_9$ ceramic powders were prepared by co-precipitation method using the way very similar to those employed for Ho-doped $SrBi_2Nb_2O_9$ presented in our previous work [10] and proposed by Okubo and Kakihana [11]. The process is depicted in flowchart of Fig. 1. The obtained precursor powders were calcined at 800 °C for 12 h and used to fabricate the $SrBi_{2-x}Eu_xNb_2O_9$ ($x = 0$, 0.4) ceramics. Ceramic pellets were prepared by uniaxial pressing under ~1 t/cm² and sintered at 850 °C for 12 h. For dielectric measurements the sintered pellets were painted by silver pastes on both sides and fired at 400 °C for 1 h to form electrodes.

Phase identification of the ceramic powders was carried out by X-ray diffraction (XRD) instrument X'Pert Pro-Panlytical. Fourier transform infrared spectroscopy (FTIR) was performed by KBr-pellet/ Bruker, Vertex 70 DTGS. The dielectric measurements were carried out by LCR meter Agilent 4284A (frequency range 20 Hz to 1 MHz) and AC conductivities were calculated using the formula:

$$\sigma_{AC} = \omega \cdot \varepsilon_0 \cdot \varepsilon' \cdot \tan\delta \qquad (1)$$

where ω is the angular frequency, ε' is dielectric constant, $\tan\delta$ is the dielectric loss and ε_0 is the permittivity of free space.

$SrCl_2 \cdot 6H_2O$ in distilled water

$\downarrow$

$NbCl_5$ in Ethanol

$\downarrow$

$Bi(NO_3)_3 \cdot 5H_2O$ in dilute HNO_3 $Eu(NO_3)_3 \cdot 5H_2O$ in distilled water

solution mixture

ammonia pH>9   precipitation, washing and drying
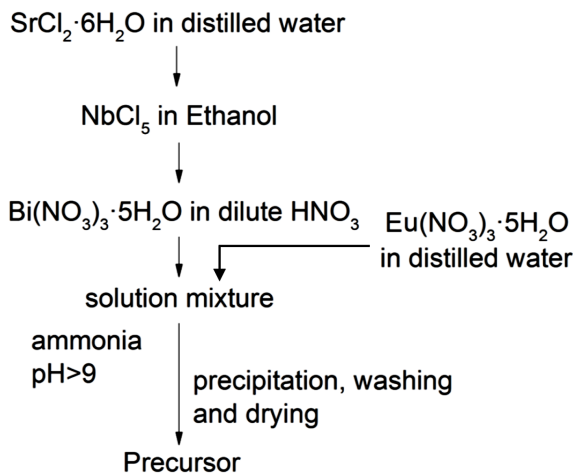
Precursor

Figure 1. Flowchart for the preparation of precursor powders

III. Results and discussions

Figure 2 shows XRD patterns of the $SrBi_2Nb_2O_9$ and $SrBi_{1.6}Eu_{0.4}Nb_2O_9$ ceramic powders. Both samples show single phase of $SrBi_2Nb_2O_9$ (JCPDS card № 01-089-8154), concluding that these phases are crystallized in an orthorhombic structure. The lattice parameters (a, b, c and V) calculated by UnitCell program are summarized in Table 1. All these parameters slightly decrease when introduced Eu in $SrBi_2Nb_2O_9$ structure, suggesting that the Eu cations have successfully diffused in the crystal lattice. Hence, the effect of Eu on lattice parameters could be correlated to the ionic radii (Bi^{3+}, 1.02 Å and Eu^{3+}, 0.95 Å [12]). Where, Eu^{3+} ions replace Bi^{3+} ions in $SrBi_2Nb_2O_9$ material, the lattice parameters are expected to be dependent on the fraction of ions replacing the original ions, and the decrease of size of ion a part being a part of a crystal leads to a directly proportional decrease of lattice parameters.
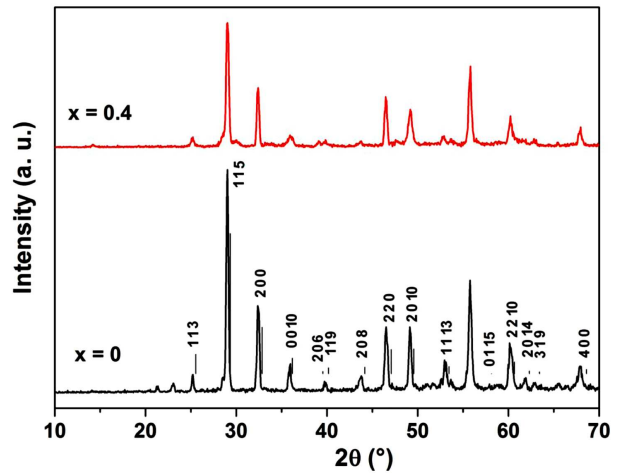

Figure 2. XRD patterns for $SrBi_{2-x}Eu_xNb_2O_9$ ($x = 0$, 0.4) ceramic powders

Figure 3 shows FTIR spectra of the $SrBi_{2-x}Eu_xNb_2O_9$ ($x = 0$, 0.4) ceramic powders. The bands at 3440 and 1633 cm⁻¹ are due to water molecules. The bands located at 2380 cm⁻¹ can be attributed to CO_2. The bands at 2853 and 2929 cm⁻¹ indicate the presence of residual organics. The bands at 806 and 622 cm⁻¹ can be attributed to the stretching of the octahedral NbO_6 [13–15].

The densities of the samples sintered at 850 °C for 12 h were found to be around 87% when measured by pycnometer.

Figure 4 shows the dielectric constant (ε') and dielectric loss ($\tan\delta$) versus temperature (of the sintered samples) at different frequencies. The undoped ceramic sample shows an increase of dielectric constant

Table 1. Lattice parameters and unit cell volume for $SrBi_{2-x}Eu_xNb_2O_9$

x	a [Å]	b [Å]	c [Å]	Unit cell volume [Å³]
0	5.50453±0.00108	5.50812±0.00028	25.09087±0.00174	760.7462±0.1412
0.4	5.49773±0.00108	5.50231±0.00028	25.07565±0.00174	758.5441±0.1406
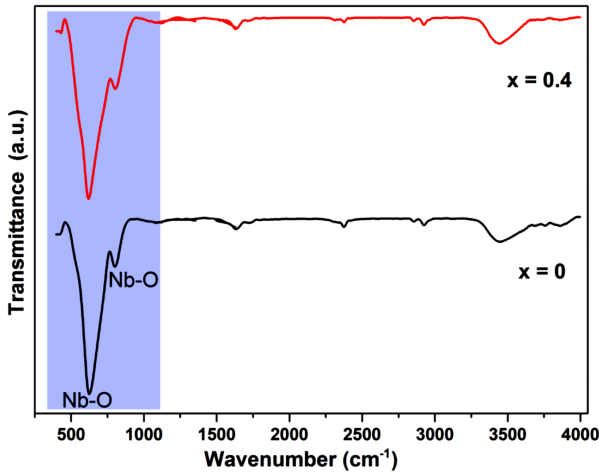
Figure 3. FTIR spectra for SrBi$_{2-x}$Eu$_x$Nb$_2$O$_9$ ($x = 0, 0.4$) ceramic powders

with the increasing of temperature, followed by a peak at ~420 °C (corresponding to the Curie temperature), which is not influenced by the frequency. However, Eu-doping results in the appearance of a board peak (at ~400 °C), probably caused by the inhomogeneous distribution of europium in the layered structure [16,17]. The temperature dependence of the dielectric loss (Fig. 4) of both ceramics reveals a significant increase of tan δ

from 50 °C up to a local maximum. The observed broad maxima are not far from the peaks recorded in ε'-T plots and correspond to the transition from ferroelectric to paraelectric phase. It is also noted a decrease of tan δ in the limited temperature range (20–50 °C) and could be attributed to the water molecular dipole moment. It is known that the dielectric properties of SrBi$_2$Nb$_2$O$_9$ material are attributed to the lone pair electrons on Bi^{3+} and the oxygen vacancies resulting from the volatilization of bismuth at high temperatures [18]. However, the incorporation of europium into SrBi$_2$Nb$_2$O$_9$ structure results in a slight enhancement of ε' and tan δ. The reason for the observed behaviour of the doped sample could be attributed to the insulating grain boundary layers formed by diffusion of defects [19,20]. As temperature increases, the contribution of extrinsic defect dipoles diminishes (for the doped ceramics) in favour of motion of oxygen vacancies (for the undoped ceramics).

The Curie temperature of the SrBi$_2$Nb$_2$O$_9$ sample (~420 °C) is slightly lower than those reported for SrBi$_2$Nb$_2$O$_9$ (~440 °C) ceramics prepared by solid state method [21] but it is slightly higher in comparison with TC of the doped one (~400 °C). The small decrease of the Curie temperature with Eu doping may be caused by changes in Nb−O−Nb angles, leading to a smaller rattling space for the Nb ions inside the oxygen octahedron
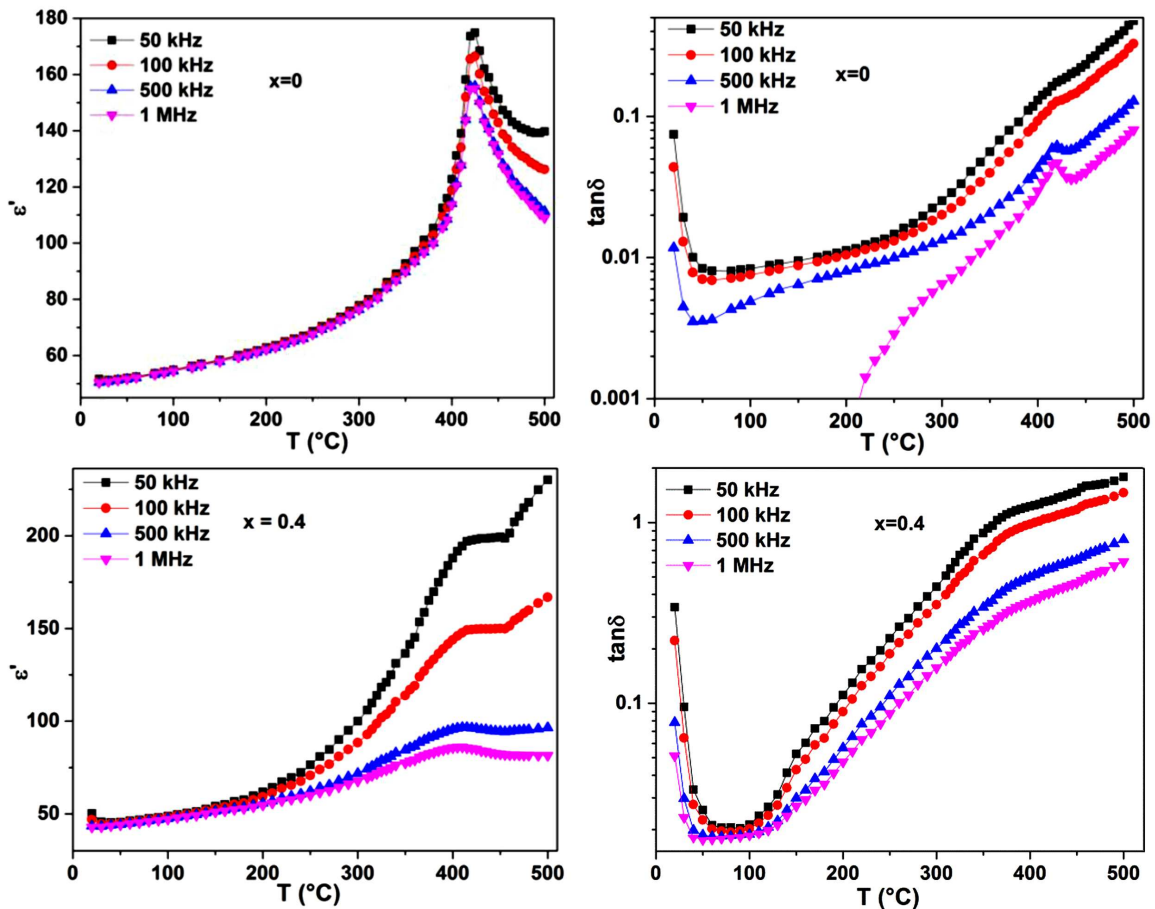

Figure 4. Dependence of dielectric constant (ε') ant dielectric loss (tanδ) on temperature of SrBi$_{2-x}$Eu$_x$Nb$_2$O$_9$ ($x = 0, 0.4$) ceramics
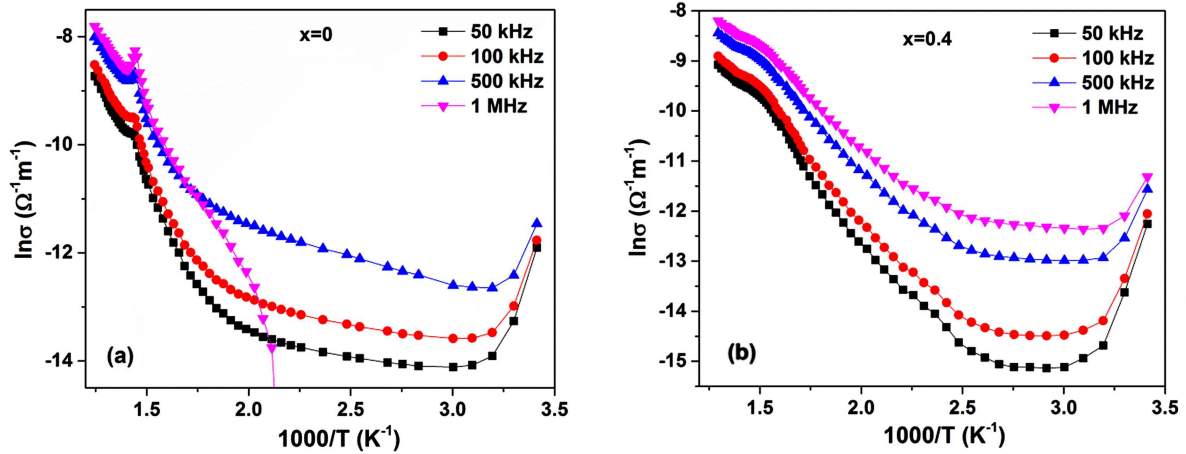
Figure 5. Reciprocal temperature dependence of the AC conductivity for: a) SrBi$_2$Nb$_2$O$_9$ and b) SrBi$_{1.6}$Eu$_{0.4}$Nb$_2$O$_9$ ceramics

NbO$_6$, which will decrease the ionic displacements and thus the Curie temperature goes down [21,22].

Figure 5 shows the temperature dependence of the electrical conductivity for SrBi$_{2-x}$Eu$_x$Nb$_2$O$_9$ ($x = 0$, 0.4) ceramics. The undoped SrBi$_2$Nb$_2$O$_9$ exhibits a lower electrical conductivity ($\sim 10^{-5}\,\Omega^{-1}\text{m}^{-1}$) at room temperature, compared to that of the doped material ($\sim 3.5 \times 10^{-5}\,\Omega^{-1}\text{m}^{-1}$), when measured at 500 kHz. The electrical conductivity of both samples slightly decreases up to 50 °C and then increases with the increasing temperature, due to the thermally activated oxygen ionic migration. Thus, the oxygen ion movement is the most common transport mechanism in Bi-based materials [6,20]. The mechanism of the formation of oxygen vacancies could be described by Kröger-Vink notation [21,22]:

$$\frac{1}{2}\,O_2 + V_O^{\bullet\bullet} + 2\,e^- \longleftrightarrow O_o$$
$$V_{Bi} + e^- \longleftrightarrow V_{Bi}^{'} \qquad (2)$$
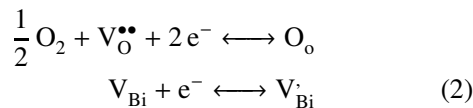
where $V_O^{\bullet\bullet}$ is the oxygen vacancy with +2 effective charge and O_O denotes oxide ion in the crystal.

The appearance of the peak on AC conductivity versus temperature plots little below 1.5 K^{-1} for the pure

SrBi$_2$Nb$_2$O$_9$ ceramics can be clearly seen (Fig. 5a). The change in the slope of the straight line occurred while passing through the Curie point showing the characteristic positive temperature coefficient of resistance (PTCR) effect. Such behaviour has been reported in La-substituted SrBi$_2$Nb$_2$O$_9$ ceramics [27,28].

Yilmaz *et al.* [29] studied electrical conductivity of Bi$_2$O$_3$ doped with Eu$_2$O$_3$. They found an increased conductivity with the increase of doping concentration and temperature. It was proposed that this is connected with the interstitial oxygen ionic migration with rises with the increasing temperature. Our results are in good agreement with this report.

Our processes based on a precipitation permits to prepare SrBi$_{1.6}$Ho$_{0.4}$Nb$_2$O$_9$ (our previous work [10]) and SrBi$_{1.6}$Eu$_{0.4}$Nb$_2$O$_9$ (present work) materials. However, reliable physic results under the same conditions have not been achieved. Thus, the electrical and dielectric behaviour of the SrBi$_{1.6}$Eu$_{0.4}$Nb$_2$O$_9$ at room temperature differs from that observed in the SrBi$_{1.6}$Ho$_{0.4}$Nb$_2$O$_9$ ceramics, where the AC conductivity, ε' and tan δ decrease as Ho substitutes for Bi.

Figure 6a shows the imaginary part of the complex modulus as a function of frequency at different temperatures for the SrBi$_{2-x}$Eu$_x$Nb$_2$O$_9$ ($x = 0$, 0.4) ceramics.
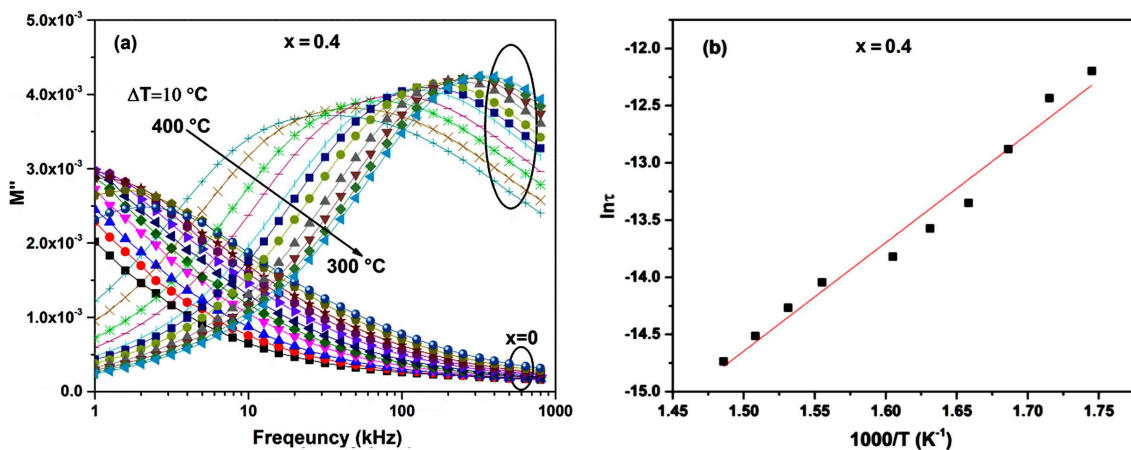

Figure 6. Variation of (a) M'' with frequency at different temperatures, and (b) Arrhenius plot of conductivity relaxation time

The electric modulus M'' was calculated from ε' and ε'' ($\varepsilon'' = \varepsilon' \cdot \tan\delta$):

$$M'' = \frac{\varepsilon''}{\varepsilon''^2 + \varepsilon'^2} \qquad (3)$$

The M'' plots are asymmetric and the peaks (M''_{max}) shift towards higher frequencies for $x = 0.4$ with increasing temperature, proving to be non-Debye type. The frequency region below M''_{max} determines the range in which charge carriers remain mobile over long distances. Above M''_{max} the carriers are confined to potential wells and mobile on short distances [25–27]. However, the relaxation M''_{max} peaks are not observed in the case $x = 0$ at selected temperatures. Maybe in the undoped sample M''_{max} peak could be observed in the low frequency region which is not presented.

Figure 6b depicts the relaxation time as a function of temperature for the doped material. The relaxation time is found to obey the Arrhenius law:

$$\tau = \tau_0 \cdot \exp\left(\frac{E_\tau}{k_B \cdot T}\right)$$

$$\tau = \frac{1}{2\pi \cdot f_{max}} \qquad (4)$$

where f_{max} is the peak frequency of M''. From the slope of the fit, the activation energy E_τ is found to be 0.81 eV. The results of conductivity and electrical modulus show thermal activation-type behaviour due to a hopping of charge carriers. That would result from a random cation distribution between $[Bi_2O_2]^{2+}$ layers and $[SrNb_2O_7]^{2-}$ perovskite-type layers [28,29].

IV. Conclusions

$SrBi_{2-x}Eu_xNb_2O_9$ ($x = 0$, 0.4) samples have been successfully prepared by co-precipitation method. The samples were confirmed to be single phase by XRD. FTIR spectroscopy does not present a displacement of the bands. There is the influence of the doping on dielectric and electrical conductivity. At room temperature, dielectric constant, dielectric loss and AC conductivity slightly increase by introducing europium in the material. The Curie temperature data show that the ferroelectric transition is classic for the undoped sample and diffuse behaviour took place for the doped one. The relaxor behaviour took place and the frequency plots of imaginary modulus suggest the relaxation to be non-Debye type with a rise of Eu content.

References

1. V.A. Isupov, "Two types of $ABi_2B_2O_9$ layered perovskite-like ferroelectrics", *Inorg. Mater.*, **43** (2007) 976–979.
2. R. Qiu, F. Zhang, S. Zheng, Y. Li, W. Zhang, "Structural stability in Aurivillius phases based on ab initio thermodynamics", *J. Phys. Chem. Solids.*, **75** (2014) 1088–1093.
3. N. Ortega, P. Bhattacharya, R.S. Katiyar, "Enhanced ferroelectric properties of multilayer $SrBi_2Ta_2O_9/SrBi_2Nb_2O_9$ thin films for NVRAM applications", *Mater. Sci. Eng. B*, **130** (2006) 36–40.
4. S. Lin, C. Jun-hao, Y. Ping-xiong, Y. Fang-yu, L. Ya-wei, F. Chu-de, M. Cao-liang, "Influence of substitution of Nd^{3+} for Bi^{3+} on structure and piezoelectric properties of $SrBi_{2-x}Nd_xNb_2O_9$ (x = 0, 01, 02 and 0.4)", *Trans. Nanoferrous Met. Soc. China*, **19** (2009) 1459–1463.
5. Z. Yao, H. Li, M. Ma, R. Chu, Z. Xu, H. Jigong, L. Guorong, "Preparation and electrical properties of $SrBi_{2-x}Sm_xNb_2O_9$ lead-free piezoelectric ceramics", *J. Mater. Sci. Mater. Electron.*, **27** (2015) 2114–2119.
6. J.S. Kim, B.C. Choi, H.K. Yang, J.H. Jeong, S.T. Chung, S.-B. Cho, "Low-frequency dielectric dispersion and electrical conductivity of pure and La-doped $SrBi_2Nb_2O_9$ ceramics", *J. Korean Phys. Soc.*, **52** (2008) 415–420.
7. M. Afqir, A. Tachafine, D. Fasquelle, M. Elaatmani, J.C. Carru, A. Zegzouti, M. Daoud, "Synthesis, structural and dielectric properties of $SrBi_{2-x}Sm_xNb_2O_9$", *Moscow Univ. Phys. Bull.*, **72** (2017) 196–202.
8. M. Afqir, A. Tachafine, D. Fasquelle, M. Elaatmani, J.-C. Carru, A. Zegzouti, M. Daoud, "Dielectric properties of gadolinium-doped $SrBi_2Nb_2O_9$ ceramics", *J. Mater. Sci. Mater. Electron.*, **29** (2018) 1289–1297.
9. D.P. Volanti, I.L. V Rosa, E.C. Paris, C.A. Paskocimas, P.S. Pizani, J.A. Varela, E. Longo, "The role of the Eu^{3+} ions in structure and photoluminescence properties of $SrBi_2Nb_2O_9$ powders", *Opt. Mater. (Amst.)*, **31** (2009) 995–999.
10. M. Afqir, A. Tachafine, D. Fasquelle, M. Elaatmani, J. Carru, A. Zegzouti, M. Daoud, "Synthesis , structural and dielectric properties of Ho-doped $SrBi_2Nb_2O_9$ prepared by co-precipitation", *Sci. China Mater.*, **59** (2016) 921–926.
11. T. Okubo, M. Kakihana, "Low temperature synthesis of Y_3NbO_7 by polymerizable complex method: Utilization of a methanol-citric acid solution of $NbCl_5$ as a novel niobium precursor", *J. Alloys Compd.*, **256** (1997) 151–154.
12. R.D. Shannon, C.T. Prewitt, "Effective ionic radii in oxides and fluorides", *Acta Crystallogr. Sect. B Struct. Sci.*, **B25** (1967) 925–945.
13. R. Ramaraghavulu, S. Buddhudu, "Ferroelectrics structural and dielectric properties of $BaBi_2Nb_2O_9$ ferroelectric ceramic powders by a solid state reaction method", *Ferroelectrics*, **460** (2014) 57–67.
14. A. Tarafder, A.R. Molla, B. Karmakar, "Enhanced photoluminescence and structure of Dy^{3+}-doped $SrBi_2Ta_2O_9$-containing transparent glass-ceramics", *Opt. Mater. (Amst.)*, **35** (2013) 1549–1556.
15. N.L.A. Junior, A.Z. Simoes, A.A. Cavalheiro, S.M. Zanetti, E. Longo, J.A. Varela, "Structural and microstructural characterization of $SrBi_2(Ta_{0.5}Nb_{0.48}W_{0.02})_2O_9$ powders", *J. Alloys Compd.*, **454** (2008) 61–65.
16. M. Adamczyk, Z. Ujma, M. Pawełczyk, "Dielectric properties of $BaBi_2Nb_2O_9$ ceramics", *J. Mater. Sci.*, **41** (2006) 5317–5322.
17. Y. González-Abreu, A. Peláiz-Barranco, E.B. Araújo, A.F. Júnior, "Dielectric relaxation and relaxor behavior in bilayered perovskites", *Appl. Phys. Lett.*, **94** (2009) 92–95.
18. I. Coondoo, A.K. Jha, S.K. Agarwal, "Structural, dielectric and electrical studies in tungsten doped $SrBi_2Ta_2O_9$ ferroelectric ceramics", *Ceram. Int.*, **33** (2007) 41–47.
19. S. Khasa, P. Singh, S. Sanghi, N. Singh, A. Agarwal, "Structural analysis and dielectric characterization of Aurivillius type $CaSrBi_2Nb_2O_9$ ceramics", *J. Integr. Sci.*

Technol., **2** (2014) 13–21.

20. B.P. Mandal, P. Anithakumari, S. Nigam, C. Majumder, M. Mohapatra, A.K. Tyagi, "Enhancement of dielectric constant in a niobium doped titania system: an experimental and theoretical study", *New J. Chem.*, **40** (2016) 9526–9536.

21. S. Huang, C. Feng, L. Chen, X. Wen, "Dielectric properties of $SrBi_{2-x}Pr_xNb_2O_9$ ceramics (x = 0, 0.04 and 0.2) ", *Solid State Commun.*, **133** (2005) 375–379.

22. L. Sun, J. Hao Chu, P. Xiong Yang, F. Yu Yue, Y. Wei Li, C. De Feng, C. Liang Mao, "Influence of substitution of Nd^{3+} for Bi^{3+} on structure and piezoelectric properties of $SrBi_{2-\chi}Nd_\chi Nb_2O_9$ (χ = 0, 0.1, 0.2 and 0.4)", *Trans. Nonferrous Met. Soc. China*, **19** (2009) 1459–1463.

23. B. Yang, L. Wei, Z. Wang, S. Kang, "Electrical characterization induced by structural modulation in $(Ca_{0.28}Ba_{0.72})_{2.5-0.5x}(Na_{0.5}K_{0.5})_x Nb_5O_{15}$ ceramics", *J. Electron.*, **45** (2016) 104–115.

24. A.C. Palanduz, D.M. Smyth, "Defect chemistry and charge transport in $SrBi_2Nb_2O_9$", *J. Electroceram.*, **11** (2003) 191–206.

25. W. Wang, D. Shan, J.B. Sun, X.Y. Mao, X.B. Chen, "Aliovalent B-site modification on three- and four-layer Aurivillius intergrowth", *J. Appl. Phys.*, **103** (2008) 044102.

26. F. Rehman, L. Wang, H.B. Jin, P. Ahmad, Y. Zhao, J.B. Li, "Dielectric relaxation and electrical properties of $Sm_{0.5}Bi_{4.5}Ti_3FeO_{15}$ ceramics", *J. Alloys Compd.*, **709** (2017) 686–691.

27. V. Shrivastava, A.K. Jha, R.G. Mendiratta, "Structural and electrical studies in La-substituted $SrBi_2Nb_2O_9$ ferroelectric ceramics", *Physica B*, **371** (2006) 337–342.

28. M. Afqir, A. Tachafine, D. Fasquelle, M. Elaatmani, J.C. Carru, A. Zegzouti, M. Daoud, "Dielectric properties of $SrBi_{1.8}RE_{0.2}Nb_2O_9$ (RE = Yb, Tm, Tb, Gd, Er, Sm and Ce) ceramics", *Solid State Sci.*, **73** (2017) 51–56.

29. S. Yilmaz, O. Turkoglu, M. Ari, I. Belenli, "Electrical conductivity of the ionic conductor tetragonal $(Bi_2O_3)_{1-x}(Eu_2O_3)_x$", *Cerâmica*, **57** (2011) 185–192.

30. Z. Peng, Q. Chen, D. Liu, Y. Wang, D. Xiao, J. Zhu, "Evolution of microstructure and dielectric properties of (LiCe)-doped $Na_{0.5}Bi_{2.5}Nb_2O_9$ Aurivillius type ceramics", *Curr. Appl. Phys.*, **13** (2013) 1183–1187.

31. L. Singh, U.S. Rai, A. Kumar, K.D. Mandal, "Dielectric behavior of $CaCu_3Ti_4O_{12}$ electro-ceramic doped with La, Mn and Ni synthesized by modified citrate-gel route", *J. Adv. Ceram.*, **2** (2013) 119–127.

32. C. Bharti, M.K. Das, A. Sen, S. Chanda, T.P. Sinha, "Rietveld refinement and dielectric relaxation of a new rare earth based double perovskite oxide: $BaPrCoNbO_6$", *J. Solid State Chem.*, **210** (2014) 219–223.

33. C. Long, Q. Chang, Y. Wu, W. He, Y. Li, H. Fan, "New layer-structured ferroelectric polycrystallines, $Na_{0.5}Nd_xBi_{4.5-x}Ti_4O_{15}$: Crystal structures, electrical properties and conduction behaviors", *J. Mater. Chem. C*, **3** (2015) 8852–8864.

34. Y. Zhao, H. Fan, Z. Liu, G. Liu, X. Ren, "Ferroelectric, piezoelectric properties and magnetoelectric coupling behavior in Aurivillius $Bi_5Ti_3FeO_{15}$ multiferroic nanofibers by electrospinning", *J. Alloys Compd.*, **675** (2016) 441–447.